Supplementary information for Nanotube ferroelectric tunnel junctions with giant tunneling electroresistance ratio

Jiu-Long Wang, Yi-Feng Zhao, Wen Xu, Jun-Ding Zheng, Ya-Ping Shao, Wen-Yi Tong*, Chun-Gang Duan*

AUTHOR INFORMATION

Corresponding Author

Wen-Yi Tong - Key Laboratory of Polar Materials and Devices (MOE), Ministry of Education, Department of Electronics, East China Normal University, Shanghai, 200241, China

Shanghai Center of Brain-inspired Intelligent Materials and Devices, East China Normal University, Shanghai 200241, China

E-mail: wytong@ee.ecnu.edu.cn

Chun-Gang Duan - Key Laboratory of Polar Materials and Devices (MOE), Ministry of Education, Department of Electronics, East China Normal University, Shanghai, 200241, China

Shanghai Center of Brain-inspired Intelligent Materials and Devices, East China Normal University, Shanghai 200241, China

E-mail: cgduan@clpm.ecnu.edu.cn

Authors

Jiu-Long Wang - Key Laboratory of Polar Materials and Devices (MOE), Ministry of Education, Department of Electronics, East China Normal University, Shanghai, 200241, China

Shanghai Center of Brain-inspired Intelligent Materials and Devices, East China Normal University, Shanghai 200241, China

Yi-Feng Zhao - Key Laboratory of Polar Materials and Devices (MOE), Ministry of Education, Department of Electronics, East China Normal University, Shanghai, 200241, China

Shanghai Center of Brain-inspired Intelligent Materials and Devices, East China Normal University, Shanghai 200241, China

Wen Xu - Key Laboratory of Polar Materials and Devices (MOE), Ministry of Education, Department of Electronics, East China Normal University, Shanghai, 200241, China

Shanghai Center of Brain-inspired Intelligent Materials and Devices, East China Normal University, Shanghai 200241, China

Jun-Ding Zheng - Key Laboratory of Polar Materials and Devices (MOE), Ministry of Education, Department of Electronics, East China Normal University, Shanghai, 200241, China

Shanghai Center of Brain-inspired Intelligent Materials and Devices, East China Normal University, Shanghai 200241, China

Ya-Ping Shao - Key Laboratory of Polar Materials and Devices (MOE), Ministry of Education, Department of Electronics, East China Normal University, Shanghai, 200241, China

Shanghai Center of Brain-inspired Intelligent Materials and Devices, East China Normal University, Shanghai 200241, China

Band Structure of 30ZN

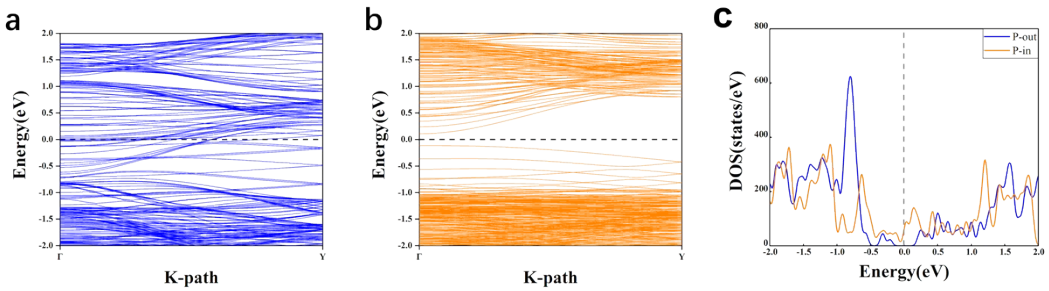

Figure S1. (a-b) The band structures of P-out and P-in 30ZN. (c) The density of state (DOS) of monolayer In_2Se_3 P-out and P-in ZN using LDA pseudopotentials.

We calculated the band structure of 30ZN. It is obviously that when the polarization is outward, band gap would close; while it opens a band gap of 0.22eV when the polarization turns inward. And the DOS of LDA also tell us the robust metal-insulator phase transition.

Properties of other In_2Se_3 nanotubes

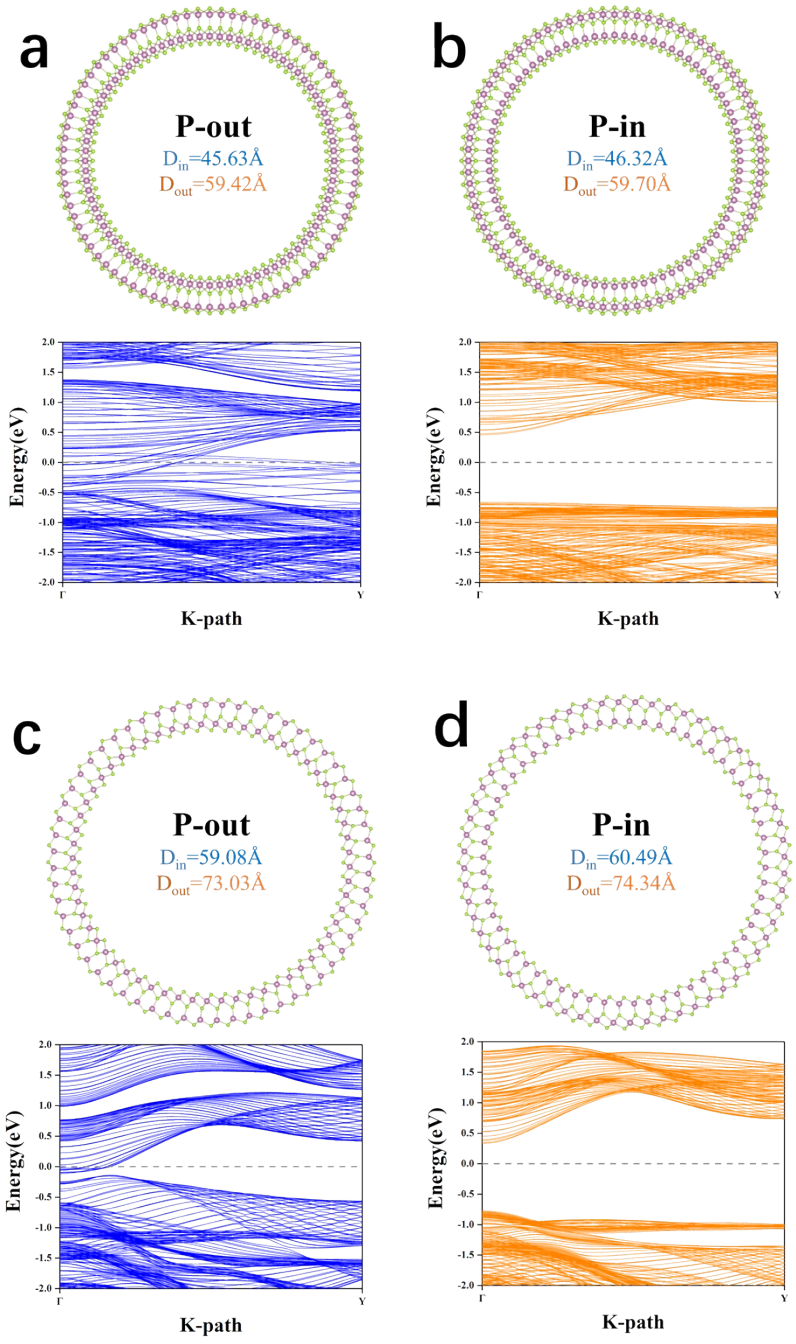

Figure S2. Schematic diagram and band structure of (a-b) P-out and P-in 40ZN, (c-d) P-out and P-in armchair nanotube with 30 units (30AN).

The structure of 40ZN and 30AN are revealed in Fig.S2(a-d), it can be seen D_{in} and D_{out} increase with the reversal of the polarization from outward to inward. P-in 40ZN opens a band gap of 1.10eV, and the band gap in P-in 30AN is 1.12eV. The P-out states, as expected, always maintain metallic. These results indicate that the metal-insulator

transition seems to be a robust feature in both zigzag and armchair In_2Se_3 nanotubes within reasonable diameters.

Transportation along radial direction

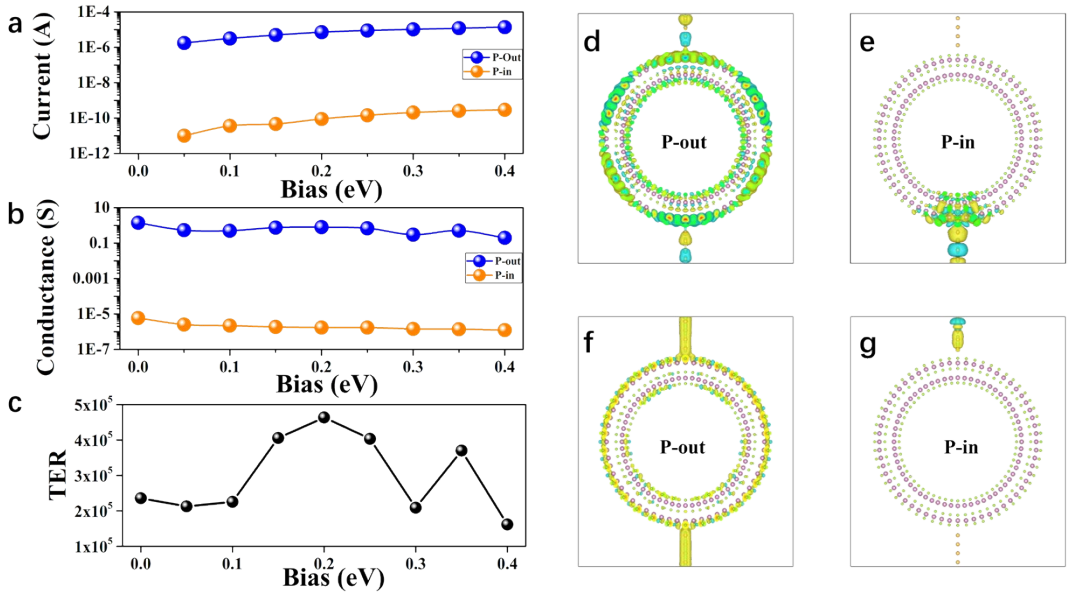

Figure S3. (a) I-V characteristic curve. (b) the conductance and (c) tunneling resistance ratio of In_2Se_3 ZN under bias. (d,e) The transport channel and (f,g) current in real space of P-out and P-in ZN with Au chain as lead under 0.15eV bias.

Without bias as shown in Fig.S4(b), the conductance of P-out 30ZN is G_{out} = 1.40 *S*; by the contrast, $G_{in} = 5.93\times10^{-6}$ *S* of P-in state is negligible. Order of magnitudes difference between two polarization states exhibits in the I-V curve of Fig.S4(a) as well. We then choose ZN under 0.15 eV bias, as example, to graphically show the change of transport channel and current in real space between P-in and P-out states. The consistency of current and transport channel confirms the metallicity in P-out nanotube (see Fig.S4(d,f)). Due to its insulating property, the P-in nanotube shows neither transport nor current channel in Fig.S4(e,g).

DOS of different units in nanotube

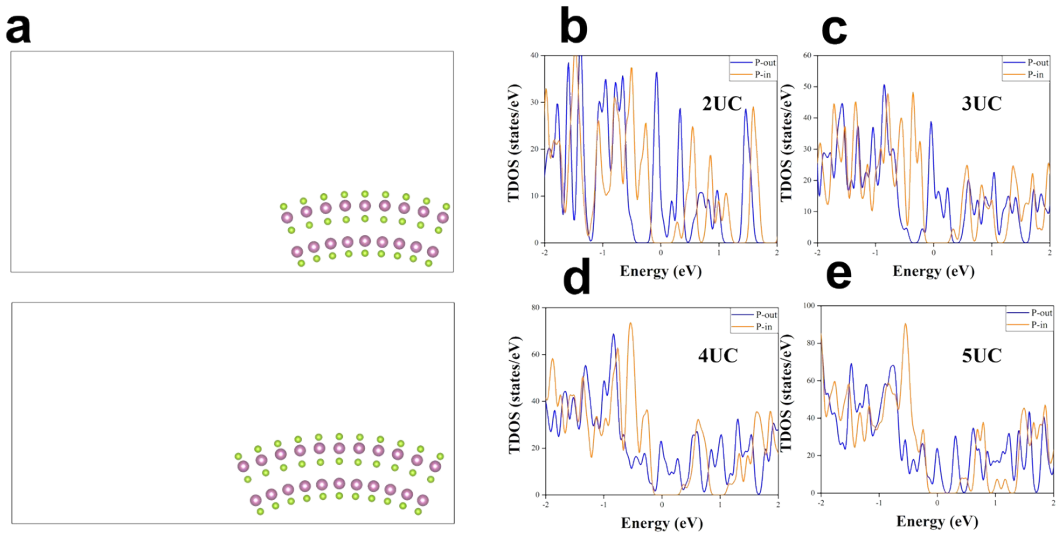

Figure S4. (a) Schematic diagram of four and five unit cells (UC) in P-in 30ZN. Vacuum are perpendicular to transport direction. (b-e) DOS of different unit cells in 30ZN.

The metal-insulator transition of α-In_2Se_3 nanotubes is robust, regardless of the number of unit cells taken into account. Moreover, the band gap of unit cells in P-in 30ZN is approximately 0.5eV. Thus, we anticipate that the ultrahigh TER ratio is an intrinsic property of ferroelectric In_2Se_3 nanotubes

DOS of nanotube FTJ

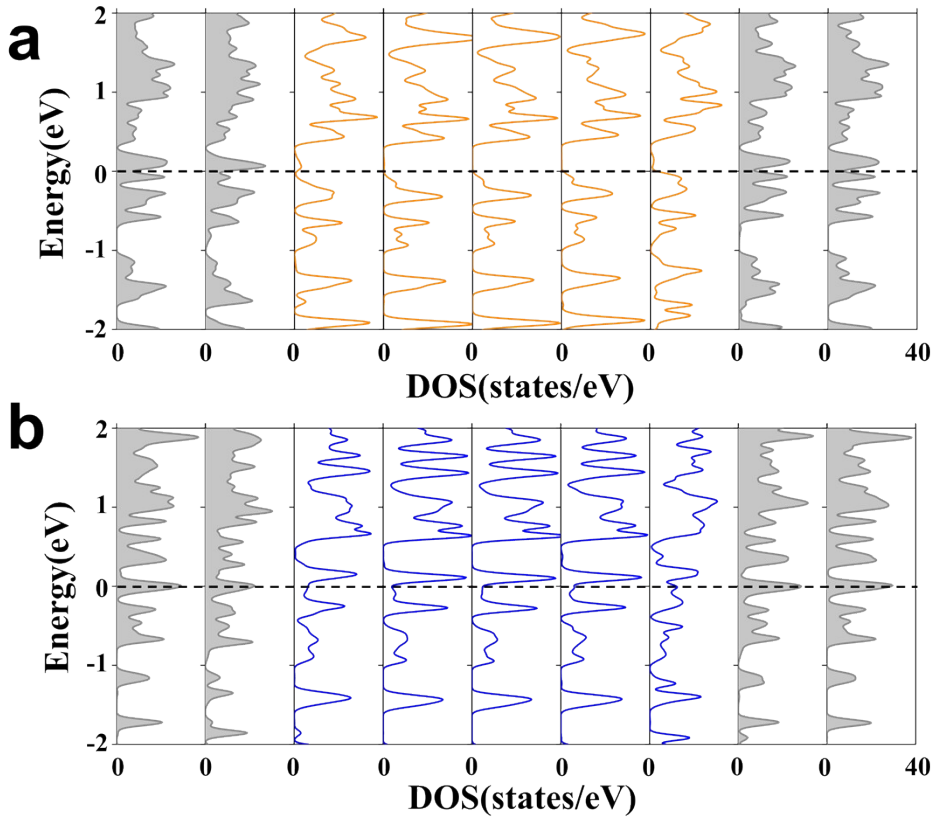

Figure S5. The layer-resolved projected density of states (PDOS) of the central region of the nanotube FTJ for (a) the P-in state, (b) the P-out state.

To study the origin of the giant TER ratio, we analyze the layer-resolved projected density of states of axial transport model, as shown in Fig.S5. In the P-out case, each layer is metallic and no gap is found around the Fermi level. In contrast, in the P-in case, there is a large band gap above the Fermi level and the Fermi level just cuts the tail of the valence band of In_2Se_3.

Some other figures

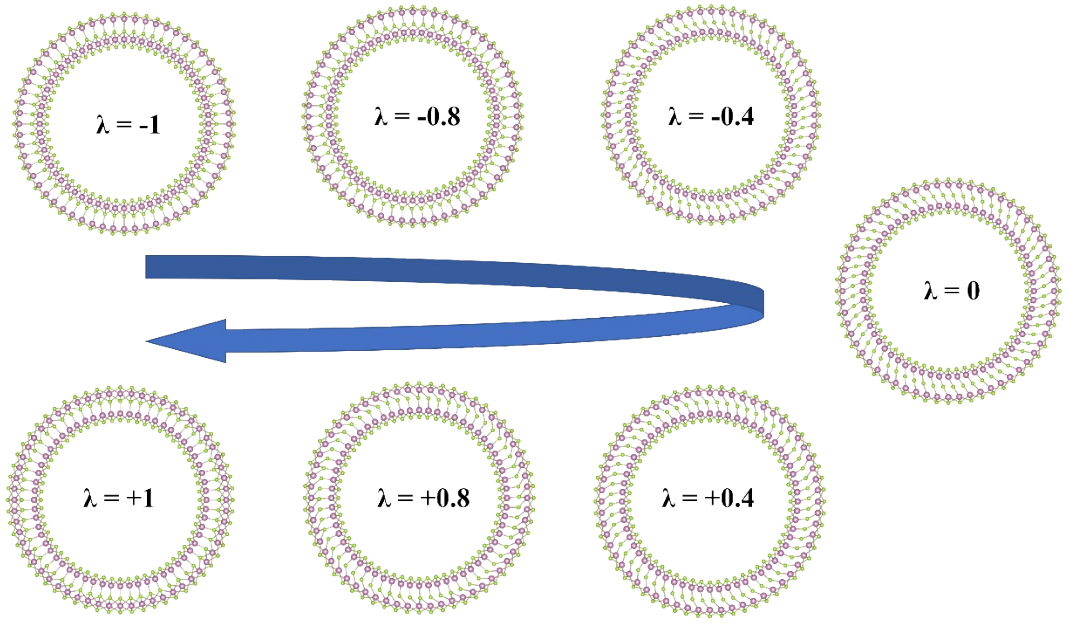

Figure. S6. Top are the structures of fcc' In_2Se_3 (β-In_2Se_3) nanotube, bottom are the structures of FE-ZB' In_2Se_3 (α-In_2Se_3) nanotube. From left to right are the structure of In_2Se_3 unit cell, top view and side view of In_2Se_3 nanotube

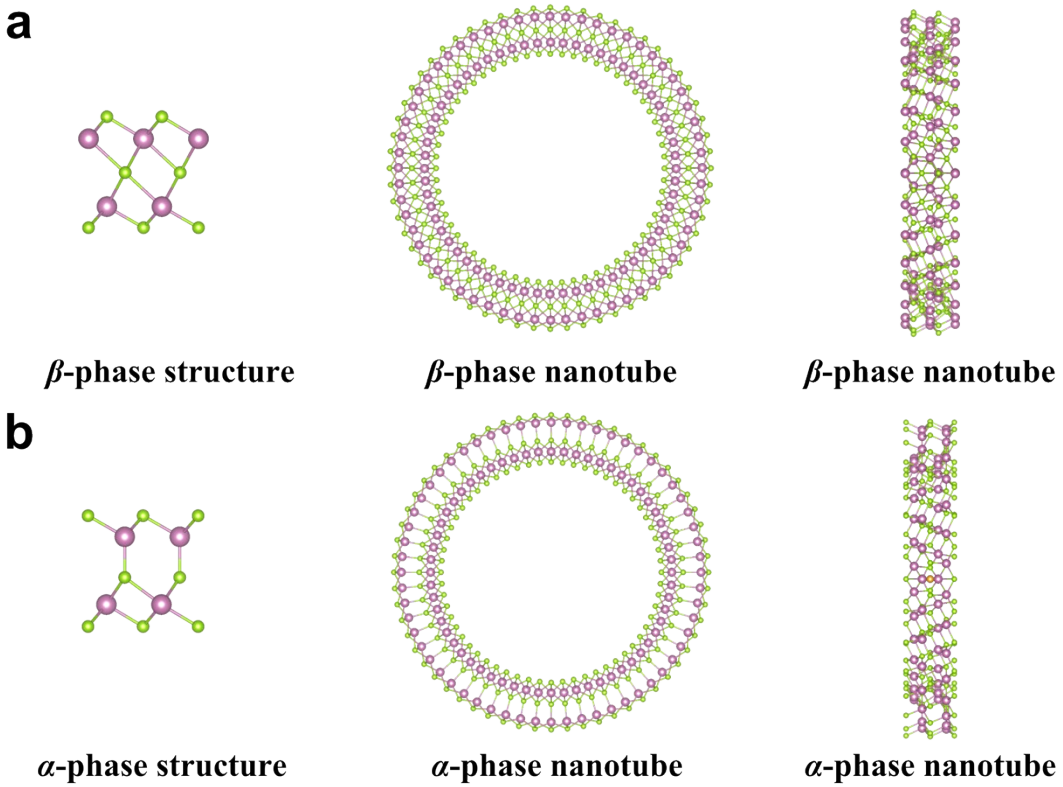

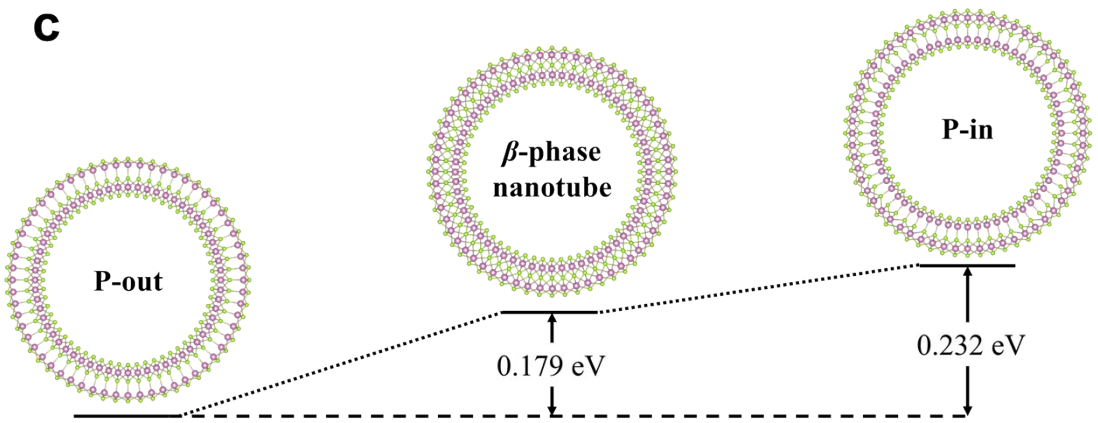

Figure. S7. The comparison of β-In_2Se_3 nanotube and α-In_2Se_3 nanotube. (a) The structures of β-In_2Se_3 nanotube. (b) The structures of α-In_2Se_3 nanotube. From left to right are the structure of In_2Se_3 unit cell, top view and side view of In_2Se_3 nanotube. (c) Kinetics pathways of polarization reversal processes with β-In_2Se_3 nanotube as transition states.

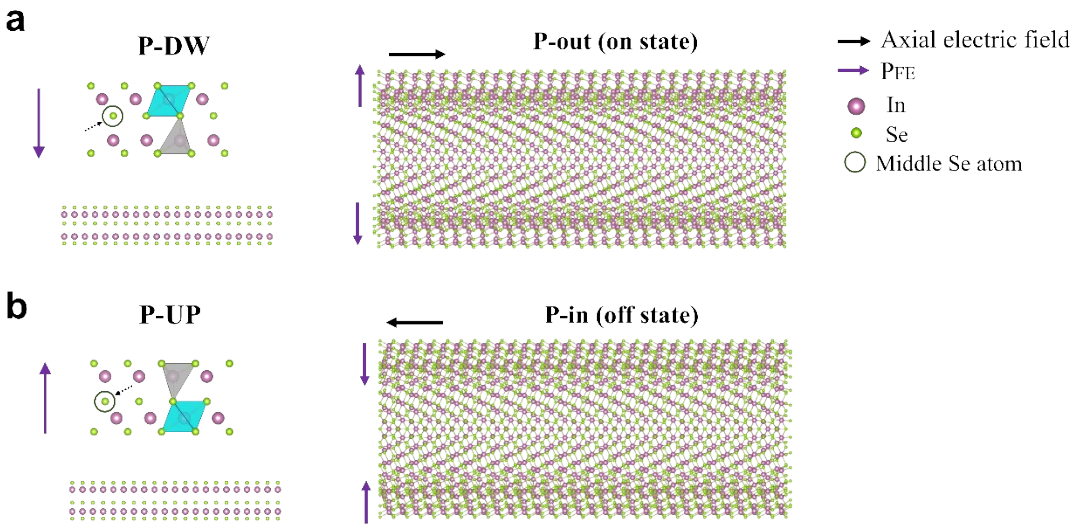

Figure. S8. (a-b) Schemetic diagram of P-DW/P-UP monolayer α-In_2Se_3 and P-out/P-in α-In_2Se_3 nanotube, the black arrows represent the axial electric fields, which can move the middle Se from left to right/right to left, and reverse the out-of-plane polarization in monolayer (radial polarization in nanotube).